

The extinction law in high redshift galaxies¹

J.A. Muñoz¹, E.E. Falco², C.S. Kochanek³, B.A. McLeod⁴ and E. Mediavilla⁵

¹*Departamento de Astronomía y Astrofísica, Universidad de Valencia, E-46100 Burjassot, Valencia, Spain*

²*F. L. Whipple Observatory, Smithsonian Institution, P. O. Box 97, Amado, AZ 85645, USA*

³*Department of Astronomy, The Ohio State University, Columbus, OH 43210, USA*

⁴*Harvard-Smithsonian Center for Astrophysics, 60 Garden St., Cambridge, MA 02138, USA*

⁵*Instituto de Astrofísica de Canarias, E-38200 La Laguna, Tenerife, Spain*

email: jmunoz@uv.es

ABSTRACT

We estimate the dust extinction laws in two intermediate redshift galaxies. The dust in the lens galaxy of LBQS 1009–0252, which has an estimated lens redshift of $z_l \simeq 0.88$, appears to be similar to that of the SMC with no significant feature at 2175Å. Only if the lens galaxy is at a redshift of $z_l \simeq 0.3$, completely inconsistent with the galaxy colors, luminosity or location on the fundamental plane, can the data be fit with a normal Galactic extinction curve. The dust in the $z_l = 0.68$ lens galaxy for B 0218+357, whose reddened image lies behind a molecular cloud, requires a very flat ultraviolet extinction curve with (formally) $R_V = 12 \pm 2$. Both lens systems seem to have unusual extinction curves by Galactic standards.

Subject headings: cosmology: observations — gravitational lensing — dust, extinction — galaxies: ISM

¹Based on observations made with the NASA/ESA Hubble Space Telescope. The Space Telescope Science Institute is operated by the Association of Universities for Research in Astronomy, Inc. under NASA contract NAS 5-26555.

1. Introduction

Precise measurements of extinction curves are almost exclusively limited to the Galaxy, the LMC and the SMC, because at greater distances it becomes impossible to obtain the photometry or spectroscopy of individual stars needed for accurate extinction law measurements. Galactic extinction curves are well fitted by parameterized models with $R_V \simeq 3.1$ ($A_\lambda \equiv R_\lambda E(B-V)$), e.g. Savage & Mathis 1979, Fitzpatrick & Massa 1988, Cardelli, Clayton & Mathis 1989, hereafter CCM), although lines of sight with dense molecular gas can show much higher values (e.g. Jenniskens & Greenberg 1993) for a total range of $2.1 < R_V < 5.8$ (see e.g. Draine 2003 and references therein). In the Galaxy and most of the Large Magellanic Cloud (LMC), the changes in the extinction law are strongly correlated with changes in the width and amplitude of the 2175Å feature in the extinction curve. The extinction curve of the Small Magellanic Cloud (SMC) and some regions of the LMC is very different from the typical Galactic extinction law in having a far weaker or nonexistent 2175Å feature (e.g. Misselt et al. 1999, Gordon et al. 2003). Physically, the extinction law depends on the mean size and composition of the dust grains along the line of sight (e.g. Clayton et al. 2003, Draine & Malhotra 1993, Rouleau et al. 1997), so it should not be surprising that it varies with the environment.

There are only fragmentary data on the extinction curves in other local galaxies. A range of R_V are found in M31, and the variations may be correlated with the local metallicity (Hodge & Kennicutt 1982, Iye & Richter 1985). There is evidence that the extinction curves of early-type galaxies are steeper functions of λ^{-1} , but there are no cleanly measured extinction curves (Warren-Smith & Berry 1983, Brosch & Loinger 1991, Goudfrooij et al. 1994). At least in the optical (I-band through B-band), Riess et al. (1996) used Type Ia supernovae to show that the extinction curves of nearby galaxies were consistent with a mean optical extinction curve having $R_V = 2.6 \pm 0.3$. In short, aside from one spiral galaxy and two irregulars (the Galaxy, the LMC and the SMC) we have few quantitative measurements of dust properties.

The galaxies, that have been studied so far, are not a representative sample of galaxies or environments. Moreover, all the physics governing dust properties (metallicity, star formation and evolution rates, radiation backgrounds) evolve strongly with redshift, so we would expect the properties of the dust to evolve with redshift. Evolution in the mean extinction law with redshift would be a crucial systematic uncertainty in studies of Type Ia supernovae to constrain the cosmological model (see, e.g., Perlmutter et al. 1999), since extinction modifies the apparent stretch of the light curves (Nugent et al. 2002). Extinction laws are also required for models of galaxy evolution (e.g., in semi-analytic models, Silva et al. 2001, or population synthesis models, Gordon et al. 1997), for estimates of star formation rates in

individual galaxies (e.g. Pettini et al. 1998; Meurer et al. 1999) or to construct a global history of star formation (e.g. Madau et al. 1998; Steidel et al. 1999). Extinction also affects the light curves of γ -ray bursts (e.g. Price et al. 2001, Jha et al. 2001), and deriving the extinction law from afterglows requires theoretical assumptions about the intrinsic spectrum of the burst. With the increasing need for extinction corrections at higher redshifts, it would be wise to obtain more quantitative measurements of dust properties at similar redshifts. To make any progress, we need a probe of extinction which has the precision of local stellar measurements and works at $z = 1$ just as well as at $z = 0$.

Gravitational lenses provide a unique tool to study the extinction properties of high redshift galaxies. In most of the ~ 80 known lens galaxies we see 2 or 4 images of a background AGN produced by the deflection of light by a foreground lens galaxy. When each image's light traverses the lens galaxy, it is extinguished by the dust at that position. When the dust is not uniform, the amount of extinction is different for each image, whose observational signature is that the flux ratios of the images depend on wavelength (Nadeau et al. 1991). Extinction curves have been estimated for several systems using optical and infrared flux ratios (Nadeau et al. 1991, Jaunsen & Hjorth 1997, Motta et al. 2002, Wucknitz et al. 2003), and Falco et al. (1999) made a general survey of dust properties using the available lens photometry. Unfortunately, ground-based observations can study the region around the 2175Å feature only for the highest redshift lenses. The feature is redshifted to wavelengths above the atmospheric cutoff (3500 Å) for $z_l > 0.6$, and is easily studied only for $z_l \simeq 1$. Most photometry from Hubble Space Telescope (HST) observations is limited to the V, I and H-bands, since the observations were designed to study the lens and host galaxies rather than extinction. In this paper we used near-UV observations with the Hubble Space Telescope (HST) to study the extinction law of two gravitational lenses near the 2175Å feature. We summarize the observations in §2 and the results in §3.

2. Observations

From the Falco et al. (1999) lens extinction survey, we selected 3 lenses with significant extinction whose redshifted 2175 Å feature would lie at longer wavelengths than the Lyman limit of the source quasar (i.e. $2175(1 + z_l)$ Å $>$ $912(1 + z_s)$ Å). We used a total of 10 orbits to observe B 0218+357 (6 orbits), LBQS 1009–0252 (2 orbits) and Q 2337+0305 (2 orbits).

Table 1 shows a log of our WFPC2 observations. Each image was composed of dithered but not CR-split sub-exposures. The original observing request was reduced, and our subsequent decision to obtain data for all the proposed targets forced us to use only 2 sub-exposures for most of the observations. Unfortunately, for Q 2237+0305, we found the short

integrations insufficient to produce a useful extinction measurement and we include only the photometric results for this system. The sub-exposures were combined using standard methods (e.g. as in Lehár et al. 2000) but with additional manual masking to control the cosmic rays. Table 2 presents the magnitude measurements for all three systems.

3. Analysis and Discussion

If $m_0(\lambda)$ is the intrinsic QSO spectrum expressed as magnitudes at observed wavelength λ , then the spectrum of lensed image i , $m_i(\lambda)$, is

$$m_i(\lambda) = m_0(\lambda) - M_i + E_i R\left(\frac{\lambda}{1 + z_l}\right) \quad (1)$$

where M_i and $E_i = E(B - V)$ are the magnification and extinction of image i , and $R(\lambda/(1 + z_l))$ is the extinction curve redshifted to the lens redshift z_l . By measuring the magnitude differences as a function of wavelength for each image pair (e.g., A and B)

$$m_B(\lambda) - m_A(\lambda) = \Delta M + \Delta E R\left(\frac{\lambda}{1 + z_l}\right) \quad (2)$$

we can measure the relative magnifications $\Delta M = M_B - M_A$, extinction differences $\Delta E(B - V) = E_B(B - V) - E_A(B - V)$, and the mean extinction curve $R(V)$ without needing to know the intrinsic spectrum $m_0(\lambda)$. We assume that the shape of the source spectrum does not vary with time, that there is no wavelength dependence $M_i(\lambda)$ to the magnification due to microlensing, and that extinction curve is the same for all images. We will discuss these assumptions further below.

We used a standard χ^2 statistic to fit the model to the measurements and to determine ΔM , ΔE , R_V and their uncertainties. We used either the Cardelli et al. (1989) parameterized models for the Galactic extinction curve or the Fitzpatrick & Massa (1990) model with its parameters set to the values found by Gordon et al. (2003) for the average extinction in the SMC. The Galactic models have a strong 2175Å feature while the SMC models do not. We also attempted to determine the dust redshift z_d by varying the lens redshift z_l in our fits (Jean & Surdej 1998, Falco et al. 1999). If the wavelength dependence of the flux ratios is due to extinction, then we should find that z_d is consistent with z_l . Table 3 shows the results for these parameters.

From the colors of the lens galaxy in LBQS 1009-0252 or its location on the fundamental plane, we estimated that the lens redshift is $z_l = z_{FP} = 0.88_{-0.11}^{+0.04}$ (Kochanek et al. 2000). To date, these estimated redshifts have always been confirmed by subsequent spectroscopic

measurements. An example at similar redshift and with similar photometric data is HE1104–1805, where the Lidman et al. (2000) spectroscopic redshift of $z_l = 0.73$ exactly matched the prior prediction of $z_{FP} = 0.73 \pm 0.04$ from the fundamental plane. Fig. 1 shows the magnitude differences as a function of the observed wavelength, and there is no sign of a 2175Å feature at the $z_{FP} = 0.88$ redshifted wavelength of $\lambda^{-1} \simeq 2.45 \mu\text{m}^{-1}$. For $z_l = z_{FP}$ the best fit with a Galactic extinction curve has $\chi^2 = 32.7$. In these fits we included the H-band flux ratio from Lehár et al. (2000), although the result changes little if it is excluded. Galactic dust is permitted if the redshift estimate is wrong, as we find a perfect fit ($\chi^2 = 0.14$) with a Galactic extinction law for $z_d = 0.31 \pm 0.09$. With this low redshift, the 2175Å feature lies outside the range of our data (see Fig. 1). This is very unlikely given the colors and structural properties of the lens galaxy because it is almost impossible for a lower redshift galaxy to mimic the colors and structure of a higher redshift early-type galaxy (see Lehár et al. 2000 and Kochanek et al. 2000).

The data are, however, very well fitted ($\chi^2 = 0.65$) by an SMC extinction curve redshifted to the expected $z_l = z_{FP} = 0.88$ (see Fig. 1). The SMC extinction curves lack the features needed to estimate a dust redshift, and we can find a good fit for almost any lens redshift ($0 \lesssim z_d \lesssim 2$ at 2σ). Chromatic microlensing can also produce wavelength-dependent flux ratios (see e.g. Yonehara et al. 1999), but the lack of significant changes in the V and I flux ratios between 1999.01 and 1999.11 argues against a significant contribution from microlensing. In order to obtain such a rapid change in the flux ratio with wavelength using microlensing, the source would have to lie in a highly magnified region of the microlensing magnification pattern where the time scales would be relatively short. This is easily checked by comparing the emission line and continuum flux ratios in a spectrum, since extinction has the same effect on both spectral components while microlensing primarily affects the continuum fluxes (e.g. Wucknitz et al. 2003).

The second lens, B 0218+357, has a known spectroscopic redshift of $z_l = 0.6847$ (Browne et al. 1993, Stickel & Kuhr 1993). We combined the 6 WFPC2 flux ratios with the radio flux ratio of $m_B - m_A = 1.40 \pm 0.03$ (Biggs et al. 1999). The radio flux ratio provides a direct constraint on the true magnification ratio ΔM because it is unaffected by extinction. The magnitude differences (see Fig. 2) show a feature at the redshifted wavelength of the 2175Å feature, but the overall pattern does not correspond to a standard $R_V = 3.1$ Galactic extinction curve. The data are well fitted by the Cardelli et al. (1989) model ($\chi^2 = 0.72$) for $R_V = 12 \pm 2$. This is an extrapolation well past the upper values of $R_V \simeq 5$ actually observed in the Galaxy (see e.g. Clayton et al. 2003 and references therein), but it maintains the overall structure of the high R_V extinction curves observed in the Galaxy. In this case, the dust redshift of $z_d = 0.70 \pm 0.06$ is consistent with the spectroscopic redshift. Moreover, for B 0218+357 we did not include the Lehár et al. (2000) photometry, yet the model passes

almost exactly through the H-band point lying between the radio and optical data. This is consistent with local observations that the near-IR extinction curve is universal (e.g. Martin & Whittet 1990).

B 0218+357 is known to lie behind a molecular cloud from the existence of molecular absorption lines in the radio continuum (see e.g. Combes & Wiklind 1998). Given $A_V \sim 4$ mag, an atomic Hydrogen column density of $N(H_I) \sim 10^{21} \text{ cm}^{-2}$ (Carilli, Rupen & Yanny 1993) and molecular Hydrogen column density of between $N(H_2) \sim 2 \times 10^{22} \text{ cm}^{-2}$ (Wiklind & Combes 1995; Gerin et al. 1997) and $5 \times 10^{23} \text{ cm}^{-2}$ (Wiklind & Combes 1995; Combes & Wiklind 1997; see also Menten & Reid 1996), we find a gas to dust ratio of $N_H/A_V \sim (1 - 25) \times 10^{22} \text{ cm}^{-2} \text{ mag}^{-1}$. The uncertainties are driven by the large range of the molecular column density measurements. Gas-to-dust ratios in the Galaxy have an average value of $N_H/A_V \sim 1.87 \times 10^{21} \text{ cm}^{-2} \text{ mag}^{-1}$ (for $R_V = 3.1$, Bohlin et al. 1978) with a remarkable small scatter $\sim 30\%$. At higher R_V the value of N_H/A_V appears to be greater than the average, but the highest value measured, corresponding to ρ Ophiuchus ($R_V = 4.2$), is only twice the average (see e.g. Kim & Martin 1996). Further study will be needed to understand a potential relation between the extreme value of $R_V \sim 12$ with the huge measured N_H/A_V ratio for B 0218+357.

We explored whether adding dust with a different extinction law in front of the bluer image, B 0218+357B, would allow solutions with less extreme extinction curves. These models are under constrained, so we computed models for fixed ratios of the extinction between the two images ($E_B(B - V) = 0.25E_A(B - V)$, $0.50E_A(B - V)$ and $0.75E_A(B - V)$). The results for a particular test, using a standard Galactic $R_V = 3.1$ extinction law for the B image, are shown in Fig. 3. As we increase the extinction for image B, we find fits with lower values of R_V for image A. This behavior is generic over a wide range of choices ($2 < R_V^B < 5$) for the B image extinction curve. In the final analysis, however, this approach does not seem to be a plausible solution because models with enough extinction in the B image to allow significantly smaller values of R_V^A also imply an intrinsic source spectrum with an inverted 2175Å feature. This is not physically plausible, so it is unlikely that the B image can suffer significant extinction. These conclusions do not change if we assume an SMC-like extinction law for image B rather than a Galactic law.

In summary, both the LBQS 1009–0252 and B 0218+357 lens systems seem to have unusual extinction curves. This is not true of all lenses. Falco et al. (1999) found several systems with extinction curves reasonably consistent with standard Galactic models, and Motta et al. (2002) conclude that the lens SBS 0909+532 is fitted well by a standard $R_V = 2.1 \pm 0.9$ extinction law. There is one caveat on our results, arising from the fact that we ignored the possibility of wavelength dependent magnifications due to microlensing from

the stars in the lens galaxy (see e.g. Yonehara et al. 1999). Because the deviations from normal extinction curves are large, both systems would have to have large microlensing magnifications and correspondingly small source sizes. At least for LBQS 1009–0252 this can be checked by studying the flux ratios of the images in the emission lines and the continuum of the quasars, where they should be the same if dust is responsible for the wavelength dependence of the flux ratios and very different if microlensing is responsible. Unfortunately, the source in B 0218+357 is a BL Lac object and lacks strong optical emission lines. The flux ratios should also show time variability on time scales of 1–10 years if the cause is microlensing, and the lack of significant changes between our present results and Lehar et al. (2000) argues against microlensing.

Our results confirm the unique value of gravitational lenses for studying extinction laws at cosmological distances. Since the number of known lenses is increasing rapidly, the only barrier to further studies of extinction laws is the need for near-UV HST observations to study the region near the 2175Å feature.

Acknowledgments: JAM is a *Ramón y Cajal Fellow* from the MCyT of Spain. EEF, CSK and BAM were supported in part by the Smithsonian Institution. These observations were obtained as part of HST grant GO-8252. CSK is supported by NASA ATP grant NAG5-9265.

REFERENCES

- Biggs, A. D., Browne, I. W. A., Helbig, P., Koopmans, L. V. E., Wilkinson, P. N., & Perley, R. A. 1999, MNRAS, 304, 349
- Bohlin, R. C., Savage, B. D., & Drake, J. F. 1978, ApJ, 224, 132
- Brosch, N. & Loinger, F., 1991, A&A, 249, 327
- Browne, I. W. A., Patnaik, A. R., Walsh, D., & Wilkinson, P. N. 1993, MNRAS, 263, L32
- Cardelli, J.A., Clayton, G.C. & Mathis, J.S., 1989, ApJ, 345, 245
- Carilli, C. L., Rupen, M. P., & Yanny, B. 1993, ApJ, 412, L59
- Clayton, G. C., Wolff, M. J., Sofia, U. J., Gordon, K. D., & Misselt, K. A. 2003, ApJ, 588, 871
- Combes, F. & Wiklind, T. 1997, ApJ, 486, L79
- Combes, F. & Wiklind, T. 1998, A&A, 334, L81

- Draine, B. & Malhotra, S., 1993, *ApJ*, 414, 632
- Draine, B. T. 2003, *ARA&A*, 41, 241
- Falco, E. E. et al. 1999, *ApJ*, 523, 617
- Fitzpatrick, E.L., & Massa, D., 1988, *ApJ*, 307, 734
- Fitzpatrick, E. L. & Massa, D. 1990, *ApJS*, 72, 163
- Gerin, M., Phillips, T. G., Benford, D. J., Young, K. H., Menten, K. M., & Frye, B. 1997, *ApJ*, 488, L31
- Gordon, K. D., Calzetti, D., & Witt, A. N. 1997, *ApJ*, 487, 625
- Gordon, K. D., Clayton, G. C., Misselt, K. A., Landolt, A. U., & Wolff, M. J. 2003, *ApJ*, 594, 279
- Goudfrooij, P., de Jong, T., Hansen, L. & Norgaard-Nielsen, H.U., 1994, *MNRAS*, 271, 833
- Hodge, P.W. & Kennicutt, R.C., 1982, 87, 264
- Iye, M. & Richter, O.G., 1985, *A&A*, 144, 471
- Jaunsen, A. O. & Hjorth, J. 1997, *A&A*, 317, L39
- Jean, C. & Surdej, J. 1998, *A&A*, 339, 729
- Jenniskens, P. & Greenberg, J.M., 1993, *A&A*, 274, 439
- Jha, S., et al., 2001, *ApJL*, L155
- Kim, S. & Martin, P. G. 1996, *ApJ*, 462, 296
- Kochanek, C. S. et al. 2000, *ApJ*, 543, 131
- Lehár, J. et al. 2000, *ApJ*, 536, 584
- Lidman, C., Courbin, F., Kneib, J.-P., Golse, G., Castander, F., & Soucail, G., 2000, *A&A*, 364, L62
- Madau, P., Pozzetti, L., & Dickinson, M. 1998, *ApJ*, 498, 106
- Martin, P. G. & Whittet, D. C. B. 1990, *ApJ*, 357, 113
- Menten, K. M. & Reid, M. J. 1996, *ApJ*, 465, L99

- Meurer, G. R., Heckman, T. M., & Calzetti, D. 1999, *ApJ*, 521, 64
- Misselt, K.A., Clayton, G.C., & Gordon, K.D., 1999, *ApJ*, 515, 128
- Motta, V., Mediavilla, E., Muñoz, J.A. et al. 2002, *ApJ*, 574, 719
- Nadeau, D., Yee, H. K. C., Forrest, W. J., Garnett, J. D., Ninkov, Z., & Pipher, J. L. 1991, *ApJ*, 376, 430
- Nugent, P., Kim, A., & Perlmutter, S. 2002, *PASP*, 114, 803
- Perlmutter, S., Turner, M. S. & White, M. 1999, *PhRvL*, 83, 670
- Pettini, M. et al 1998, *ApJ*, 508, 539
- Price, P. A. et al. 2001, *ApJL*, 549, L7
- Riess, A.G., Press, W. & Kirshner, R.P., 1996, *ApJ*, 473, 588
- Rouleau, F., Henning, T. & Stognienko, R., 1997, *A&A*, 322, 633
- Savage, B.D. & Mathis, J.S., 1979, *ARA&A* 17, 73
- Silva, L., Granato, G. L., Bressan, A., Lacey, C., Baugh, C. M., Cole, S., & Frenk, C. S. 2001, *Ap&SS*, 276, 1073
- Steidel, C. C., Adelberger, K. L., Giavalisco, M., Dickinson, M., & Pettini, M. 1999, *ApJ*, 519, 1
- Stickel, M. & Kuhr, H. 1993, *A&AS*, 101, 521
- Warren-Smith, R.F. & Berry, D.S., 1983, *MNRAS*, 205, 889
- Wiklind, T. & Combes, F. 1995, *A&A*, 299, 382
- Wucknitz, O., Wisotzki, L., Lopez, S., & Gregg, M. D. 2003, *A&A*, 405, 445
- Yonehara, A., Mineshige, S., Fukue, J., Umemura, M., & Turner, E. L. 1999, *A&A*, 343, 41

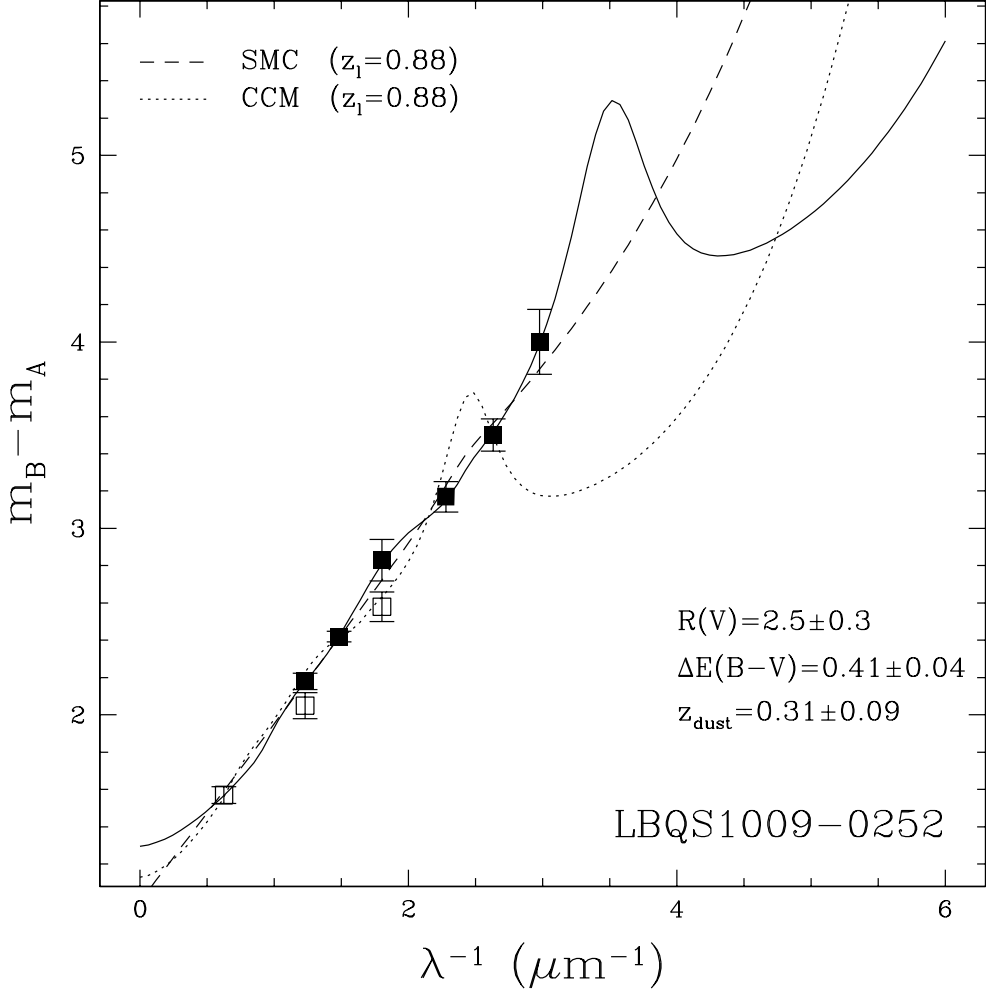


Fig. 1.— The magnitude difference as a function of observed wavelength for LBQS 1009–0252. The filled squares are the measurements from these observations and the open squares are the earlier measurements from Lehar et al. (2000). The solid line shows the best fit Galactic (CCM) extinction curve, where a redshift of $z_d \simeq 0.3$ is required to avoid predicting a 2175Å feature in the data (the dotted line shows a CCM extinction curve for a fixed $z_l = 0.88$). The dashed line shows the best fit SMC extinction law at the best estimate for the lens redshift ($z_l = z_{FP} = 0.88$) from the color, luminosity and location on the fundamental plane of the lens galaxy. The infrared data from Lehar et al. (2000) were included in the fits, although the result changes little if we use only the data from the current observations.

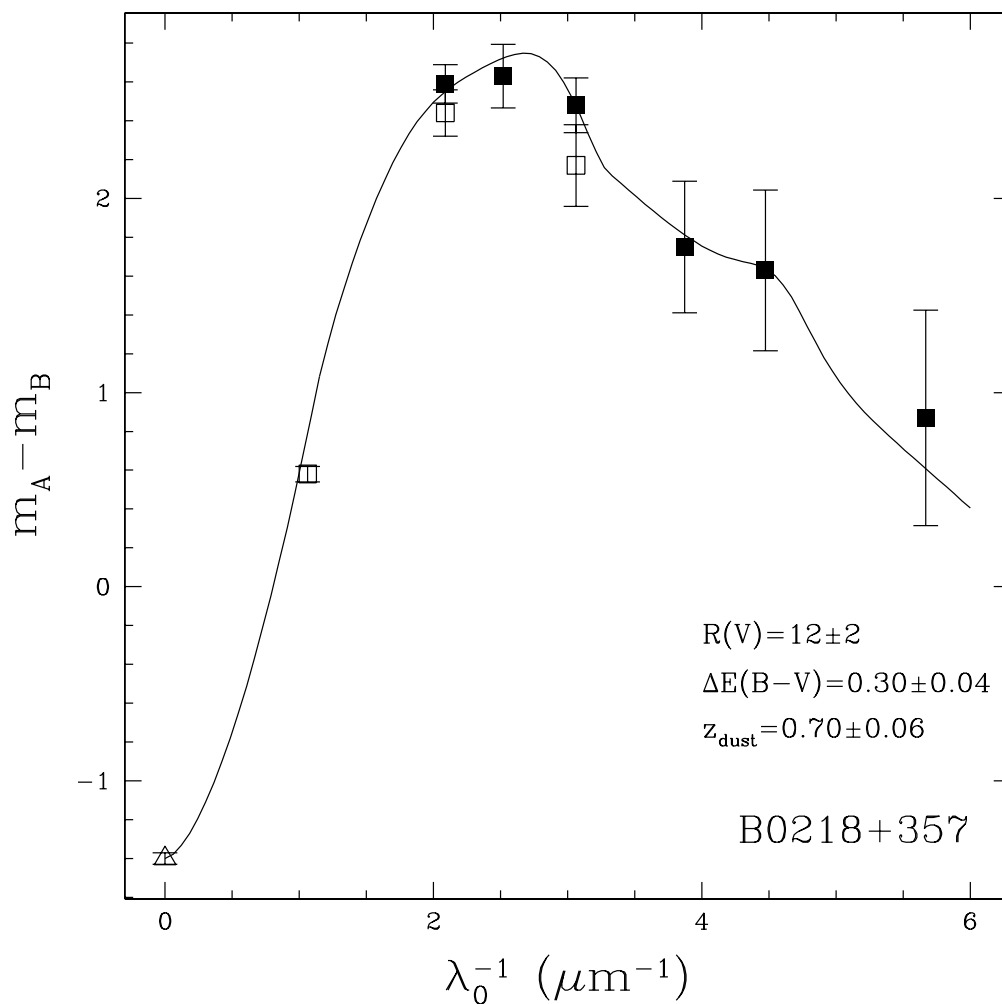


Fig. 2.— The magnitude difference as a function of the rest frame wavelength for B 0218+357. The filled squares are the measurements from these observations, the open squares are the earlier measurements from Lehár et al. (2000), and the triangle is the radio flux ratio (Biggs et al. 1999). The solid line shows the best fit Galactic (CCM) extinction curve. The Lehár et al. (1999) photometry (open squares) was not included in the fit, yet the model passes almost exactly through the H-band ($\lambda_0^{-1} = 1.06 \mu\text{m}^{-1}$) point lying between the radio and optical data.

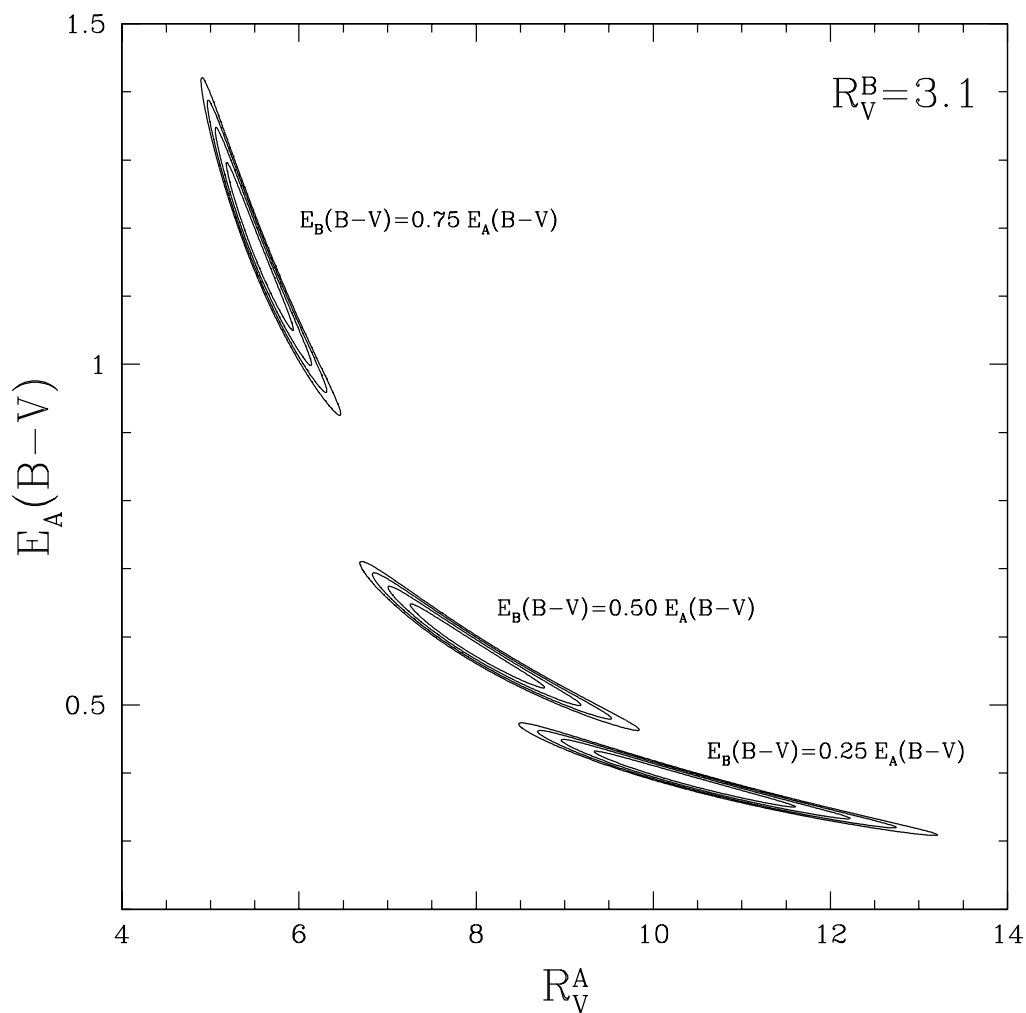


Fig. 3.— Examples of models for B 0218+357 that include extinction of the B image with a different ($R_V = 3.1$) extinction curve than is used for the A image. The χ^2 contours are shown from $\chi_{min}^2 + 1$ to $\chi_{min}^2 + 4$ assuming that $E_B(B - V)$ was fixed to be 0.75, 0.50 and 0.25 times $E_A(B - V)$.

Table 1. Log of WFPC2 Observations

TARGET	DATE-OBS (yyyy-mm-dd)	FILTER	EXP (sec)	POS. ANGLE (deg E of N)
B 0218+357	2000-03-08	F300W	3x700	100.908
B 0218+357	2000-03-08	F380W	6x1300	100.908
B 0218+357	2000-03-08	F439W	3x700	100.908
B 0218+357	2000-03-08	F555W	2x2300	100.908
B 0218+357	2000-03-08	F675W	2x180	100.908
B 0218+357	2000-03-08	F814W	2x120	100.908
LBQS 1009–0252	1999-11-05	F336W	2x500	–29.5607
LBQS 1009–0252	1999-11-05	F380W	2x350	–29.5607
LBQS 1009–0252	1999-11-05	F439W	2x180	–29.5607
LBQS 1009–0252	1999-11-05	F555W	2x60	–29.5607
LBQS 1009–0252	1999-11-05	F675W	2x60	–29.5607
LBQS 1009–0252	1999-11-05	F814W	2x60	–29.5607
Q 2337+0305	1999-10-20	F218W	2x180	123.703
Q 2337+0305	1999-10-20	F255W	2x160	123.703
Q 2337+0305	1999-10-20	F300W	2x120	123.703
Q 2337+0305	1999-10-20	F336W	2x60	123.703
Q 2337+0305	1999-10-20	F439W	2x120	123.703
Q 2337+0305	1999-10-20	F555W	2x60	123.703
Q 2337+0305	1999-10-20	F675W	2x60	123.703
Q 2337+0305	1999-10-20	F814W	2x60	123.703

Table 2. Photometry

Lens	Image	F218W	F255W	F300W	F336W	F380W	F439W	F555W	F675W	F814W	F160W
Q 2237+0305	A	17.47±0.13	16.56±0.08	16.25±0.19	15.97±0.23	...	17.00±0.10	16.95±0.15
	B	18.65±0.33	17.96±0.22	17.40±0.22	17.08±0.45	...	17.97±0.44	17.81±0.34
	C	18.96±0.32	18.24±0.27	17.72±0.29	17.48±0.20	...	18.46±0.32	18.32±0.42
	D	19.38±0.14	18.70±0.21	18.10±0.07	17.64±0.27	...	18.85±0.08	18.57±0.14
LBQS 1009-0252	A	18.28±0.05	18.78±0.09	18.77±0.02	18.41±0.07 (18.47±0.04)	18.15±0.01	17.93±0.01 (17.95±0.04)	(16.63±0.01)
	B	22.28±0.17	22.28±0.01	21.94±0.08	21.24±0.09 (21.05±0.07)	20.57±0.02	20.11±0.04 (20.00±0.06)	(18.20±0.01)
B 0218+357	A	24.40±0.50	...	24.46±0.30	24.34±0.30	23.57±0.14 (23.28±0.20)	22.78±0.16	22.01±0.10 (21.83±0.11)	(17.52±0.01)
	B	23.53±0.30	...	22.83±0.20	22.59±0.20	21.09±0.03 (21.11±0.07)	20.15±0.01	19.42±0.02 (19.39±0.05)	(16.94±0.01)

Note. — The magnitudes in parenthesis come from earlier HST observations from Lehár et al. 2000.

Table 3. Dust Properties using a CCM Extinction Curve

Lens	R(V)	$\Delta E(B - V)$	z_{dust}	z_l	ΔM	χ^2
LBQS1009-0252	2.5 ± 0.3	0.41 ± 0.04	0.31 ± 0.09	$(0.88_{-0.11}^{+0.04})^*$	1.3 ± 0.1	0.14
B0218+357	12 ± 2	0.30 ± 0.04	0.70 ± 0.06	0.6847	1.4 ± 0.3	0.72

Note. — * The spectroscopic redshift for the lens LBQS 1009-0252 is still unknown. We use the Fundamental Plane redshift estimation from Kochanek et al. (2000).